Polyhedron 29 (2010) 1015–1022

Contents lists available at ScienceDirect

Polyhedron

journal homepage: www.elsevier.com/locate/poly

1-(2′-Pyridylazo)-2-naphtholate (PAN) complexes of rhodium(III): Synthesis, structure and spectral studies

Kausikisankar Pramanik *, Basab Adhikari

Department of Chemistry, Inorganic Chemistry Section, Jadavpur University, Kolkata 700032, India

ARTICLE INFO

Article history:
Received 4 August 2009
Accepted 2 December 2009
Available online 5 December 2009

Keywords:
Rh(III) complexes
1-(2′-Pyridylazo)-2-naphthol
Crystal structures
Spectral studies
Ligand redox

ABSTRACT

The ligating properties 1-(2′-pyridylazo)-2-naphthol (HPAN) toward Rh(III) have been examined. The reaction of $RhCl_3{\cdot}3H_2O$ with HPAN in presence of excess PPh_3 afforded *trans*-$[Rh(PAN)Cl(PPh_3)_2]PF_6$ (**3PF$_6$**). Intermediate *cis*-$[Rh(PAN)Cl_2(PPh_3)]$ (**4**) has also been isolated. Solid state structures were authenticated by X-ray analyses revealing that monoanionic PAN is coordinated to rhodium in meridional fashion. Both the compounds were spectroscopically characterized in both solution and solid states, which include IR, NMR (^{1}H and ^{31}P), and optical spectra. The diamagnetic complexes show multiple CT transitions in the visible region. Low-energy transitions ($\lambda \approx 550$–650 nm) occurred in the absorption spectra are predominantly ligand centered in nature. The rhodium(III)–PAN compounds are red emissive ($\lambda_{em} \approx 650$ nm) at room temperature and the nature of the emission level is probably an ILCT level. Complexes are electro-active in acetonitrile and display irreversible oxidative and reductive waves and these responses are ascribed to be PAN ligand centered in character.

1. Introduction

The chemistry of rhodium containing multidentate ligands incorporating π-acceptor azo function is of abiding interest. Notable examples embrace the complexes of arylazothioethers [1], arylazothiolates [1], arylazophenolates [2,3], arylazoamines [4] and arylazoimines [5]. A variety of remarkable features showed by the complexes of this metal with tridentate azo ligands which include interesting coordination modes and molecular structures, potential sites of facile electron transfer, metal assisted C-hetero atom bond scission, interesting electronic structure due to the presence of low-lying π^* orbitals, photophysical behavior of delocalized transition metal chelates, and so forth. As the close environment about the metal ion governs the chemistry of the metal–ligand framework and a small change in ligand architecture can strongly influence the properties of the complexes, coordination of rhodium by azo ligands of different types has been of significant importance. It is worth noting that the structurally authenticated rhodium compounds with analogous tridentate ligands containing pyridylazo moiety are scarce [6,7].

With this background in mind, we are concerned with synthesizing new pyridylazophenolate molecules since there are only a few reports of rhodium compounds where PAN was utilized as ligand [8–11] and none of these are structurally characterized. The 1-(2′-pyridylazo)-2-naphthol ligand (HPAN, **1**) was synthesized by Tschitschibabin [12,13]. Subsequently, Cheng and Bray reported PAN as a chelating agent (metallochromic indicator) for the first time in 1955 [14]. Although, ample precedent exists for PAN as an analytical reagent for both transition and main group metals and used in qualitative as well as semiquantitative analyses [15–22], the structurally authenticated complexes are scarce and limited only to Cu(II) [23,24], Co(II and III) [25], Ru(II) [26] and Re(III) [27] centers. The first structural characterization of a copper complex was done in 1967, revealing the ligand binds to metal center via dissociation of the naphtholic proton, as a tridentate monoanionic N,N,O-donor forming two contiguous five-membered chelates (**2**) [23]. Significantly, the PAN ligand comprises two kinds of donors viz. the potent π-acceptor pyridylazo moiety and hence stabilizing low oxidation states [28–30] and the strong π-donor naphtholato-O atom, a familiar stabilizer of higher oxidation states of transition metal [31,32]. Notably, rhodium offers two stable oxidation states viz. (I) and (III), while the intermediate (II) state is unstable and highest possible (IV) state is sparse [33]. It is now of interest to recognize the valence preference of the title ligand toward rhodium.

In the present paper, we report the synthesis, spectroscopic and electrochemical properties of two rhodium(III) complexes coordinated with PAN ligand, *trans*-$[Rh(PAN)Cl(PPh_3)_2]PF_6$ (**3PF$_6$**) and *cis*-$[Rh(PAN)Cl_2(PPh_3)]$ (**4**) obtained in the reaction of $RhCl_3{\cdot}3H_2O$ with 1-(2′-pyridylazo)-2-naphthol (HPAN) in presence of PPh_3. The voltammetric data and electronic spectral assignments have also been rationalized by Density Functional Theory (DFT) calculations. The structures of both complexes have been determined by single crystal X-ray crystallography.

* Corresponding author.
E-mail address: kpramanik@hotmail.com (K. Pramanik).

0277-5387/$ - see front matter © 2009 Elsevier Ltd. All rights reserved.
doi:10.1016/j.poly.2009.12.001

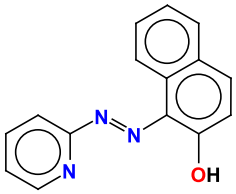

1

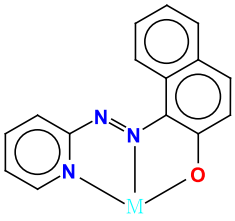

2

2. Experimental

2.1. Materials

1-(2′-Pyridylazo)-2-naphthol, triphenylphosphine and cresyl violet perchlorate were purchased from Aldrich Chemical Co. $RhCl_3{\cdot}3H_2O$ was purchased from Arora Matthey Limited and triethylamine from Merck, India. All solvents were used as received without purification. $[RhCl(PPh_3)_3]$ was synthesized by following a reported procedure [34].

2.2. Preparation of $[Rh(PAN)Cl(PPh_3)_2]PF_6$ (**3PF$_6$**)

To a 35 mL ethanolic solution of HPAN (95 mg, 0.382 mmol), triethylamine (58 mg, 0.574 mmol) was added. Then ethanolic solution (5 mL) of $RhCl_3{\cdot}3H_2O$ (100 mg, 0.380 mmol) and triphenylphosphine (400 mg, 1.527 mmol) were added successively and the mixture was refluxed for 4 h. After concentrating the volume to about 15 mL under reduced pressure, saturated ethanolic solution of NH_4PF_6 was added and stirred for 15 min to precipitate the green complex. The precipitate was filtered and washed thoroughly with water. Upon chromatographic purification of the solid on neutral silica gel (60–120 mesh) column with 5:1 toluene–acetonitrile mixture as eluent, green **3PF$_6$** was obtained. Yield 81%. *Anal.* Calc. for $C_{51}H_{40}N_3OP_3F_6ClRh$: C, 57.98; H, 3.79; N, 3.98. Found: C, 57.64; H, 3.83; N, 3.87%. IR (KBr, cm^{-1}): 1326 ν(N=N), 694 and 519 ν(Rh–P), 840 ν(P–F). ^{1}H NMR (300 MHz, $CDCl_3$): δ = 8.72 (d, J = 8.5 Hz), 7.97 (d, J = 7.9 Hz), 7.81 (t, J = 8.6 Hz), 7.67 (t, J = 8.4 Hz), 7.54 (d, J = 4.6 Hz), 7.49–7.42 (m), 7.33–7.16 (m), 6.48 (t, J = 6.5 Hz), 6.43 (d, J = 9.4 Hz). ^{31}P NMR (161.92 MHz, $CDCl_3$): δ = 19.43 (d, $^1J_{Rh-P}$ = 87.4 Hz, PPh$_3$), −144.07 (septet, $^1J_{P-F}$ = 725.4 Hz, PF_6^-).

2.3. Preparation of $[Rh(PAN)Cl_2(PPh_3)]$ (**4**)

To a 40 mL ethanolic solution of HPAN (95 mg, 0.382 mmol), triethylamine (58 mg, 0.574 mmol) and triphenylphosphine (105 mg, 0.401 mmol) were added. Then ethanolic solution (5 mL) of $RhCl_3{\cdot}3H_2O$ (100 mg, 0.380 mmol) was added and the mixture was refluxed for 2 h to afford a green solution. Solvent was evaporated under reduced pressure and the solid mass was subjected to column chromatography on neutral silica gel (60–120 mesh) column. With 3:1 toluene–acetonitrile mixture as eluent, green **4** was obtained. Yield: 68%. *Anal.* Calc. for $C_{33}H_{25}N_3OPCl_2Rh$: C, 57.89; H, 3.65; N, 6.14. Found: C, 57.62; H, 3.70; N, 6.05%. IR (KBr, cm^{-1}): 1315 ν(N=N), 683 and 519 ν(Rh–P). ^{1}H NMR (300 MHz, $CDCl_3$): δ = 8.88 (d, J = 8.34 Hz), 8.25 (d, J = 5.42 Hz), 7.67 (t, J = 7.86 Hz), 7.63–7.45 (m), 7.39 (d, J = 7.72 Hz), 7.32–7.15 (m), 6.77 (t, J = 6.23 Hz), 6.71 (d, J = 9.40 Hz). ^{31}P NMR (161.92 MHz, $CDCl_3$): δ = 27.24 (d, $^1J_{Rh-P}$ = 115.0 Hz, PPh$_3$).

2.4. Conversion of **4** to **3PF$_6$**

To a 30 mL ethanolic solution of **4** (50 mg, 0.073 mmol), triphenylphosphine (40 mg, 0.152 mmol) was added and the mixture was refluxed for 4 h. After concentrating the volume to about 15 ml under reduced pressure, saturated ethanolic solution of NH_4PF_6 was added and the mixture stirred for few minutes until precipitation of the green **3PF$_6$**. Precipitate was filtered, washed thoroughly with water and chromatographic purification was made by the above procedure. Yield: 93%.

2.5. Physical measurements

^{1}H NMR spectral measurements were carried out on a Bruker FT 300 MHz spectrometer with TMS as an internal standard. ^{31}P NMR spectra were measured on a Bruker AMX 400 MHz spectrometer operating at 161.92 MHz. UV–Vis spectra were recorded on a PerkinElmer LAMBDA 25 spectrophotometer. IR spectra were recorded on a PerkinElmer L-0100 spectrometer. The elemental analyses (C, H, N) were performed with a PerkinElmer model 2400 series II elemental analyzer. Room temperature emission spectra were recorded on a PerkinElmer LS 55 Luminescence spectrometer. Electrochemical measurements were carried out at 25 °C with VersaStat II Princeton Applied Research potentiostat/galvanostat under argon atmosphere. The cell contained a Pt working electrode and a Pt wire auxiliary electrode. Tetraethylammonium perchlorate (NEt_4ClO_4) was used as supporting electrolyte and the potentials are referenced to the Ag/AgCl electrode without junction correction.

2.6. Crystallographic studies

The single crystals suitable for X-ray crystallographic analysis of both the complexes **3PF$_6$** and **4** were obtained by slow diffusion of dichloromethane solution of the complexes into hexane. X-ray intensity data for **3PF$_6$** and **4** were collected at 293 K on Bruker SMART APEX CCD diffractometer (Mo Kα, λ = 0.71073 Å). Metal atoms were located by direct methods, and the rest of the non-hydrogen atoms emerged from successive Fourier synthesis. The structures were refined by full-matrix least squares procedure on F^2. All non-hydrogen atoms were refined anisotropically. All the hydrogen atoms were included in calculated positions and were treated as riding atoms using SHELXL default parameters. Metal atoms were located and solved by direct methods using the program SHELXS-97 [35]. The refinement and all further calculations were carried out using SHELXL-97 [36]. Calculations were performed using the SHELXTL v.6.14 program package [37]. Molecular structure plots were drawn using ORTEP [38]. Thermal ellipsoids were drawn at the 35% probability level.

2.7. Computational details

All calculations were performed using Density Functional Theory (DFT) [39] with Becke's three-parameter hybrid exchange functional [40] and the Lee–Yang–Parr nonlocal correlation functional (B3LYP) [41]. The atomic coordinates of all the complexes were taken from their X-ray structures. All calculations were performed with the GAUSSIAN 03 (G03) program [42]. The 6-31+G basis set was used for carbon, nitrogen and oxygen, 6-31+G(d,p) for chlorine and phosphorus and 6-31G was used for hydrogen. LANL2DZ basis set with Hay and Wadt effective core potential [43,44] was used for rhodium. Orbital diagrams were generated at isosurface value of 0.02 using GAUSSVIEW 3.09.

3. Results and discussion

3.1. Synthesis

In the present work, which has originated from our interest in the chemistry of rhodium in different coordination environments

[1], we have chosen HPAN (**1**) as the prime ligand type. $RhCl_3{\cdot}3H_2O$ has been selected as the starting material with the expectation that metal halide alone is competent to furnish halo-phosphine analogue of $[Rh^{III}(L)Cl(PPh_3)_2]$ (L = 2-(phenylazo)thiolate, a tridentate azo ligand) in presence of PPh_3 [1]. Treatment of an alcoholic solution of $RhCl_3{\cdot}3H_2O$ with **1** and triethylamine in presence of excess PPh_3 under refluxing condition has indeed afforded $[Rh(PAN)Cl(PPh_3)_2]PF_6$ (**3PF$_6$**) as an emerald solid in good yield (Scheme 1). Presence of triethylamine ensures the deprotonation of HPAN in solution. The title ligand is coordinated as tridentate uninegative mode. Addition of NH_4PF_6 is thus needed to satisfy the primary valence of trivalent rhodium during the course of the synthesis.

It is worth noting that the formation of the cationic complex **3PF$_6$** was diminished drastically when reaction was performed with 1 equivalent of PPh_3 coligand relative to both **1** and $RhCl_3{\cdot}3H_2O$. In that case, green $[Rh(PAN)Cl_2(PPh_3)]$ compound **4** was obtained as the major product (Scheme 2). Significantly, the relative proportion of the products (**3$^+$** versus **4**) appears to be sensitive toward the sequence of addition of metal halide and triphenylphosphine in due course of the reaction to the alcoholic solution of the dye. Prior addition of PPh_3 (1 equivalent) to the metal salt always affords **4** exclusively whereas addition of PPh_3 (1 equivalent) to a previously mixed 1:1 solution of $RhCl_3$ and PAN leads to the formation of both **4** and **3$^+$** in comparable yields. Although the neutral compound **4** was not observed with $RhCl_3$ in the presence of excess PPh_3, Wilkinson's catalyst, viz. $[RhCl(PPh_3)_3]$, alone is competent to furnish **4** in analogous conditions in moderate yield; reflecting the fascination of PAN toward rhodium(III), a borderline metal center (Scheme 2) [45]. Albeit the underlying redox process is not clear to us, the plausible oxidant is most likely to be the proton [46]. Notably, the monophosphine complex **4** is converted almost quantitatively to bisphosphine analogue **3$^+$** in presence of twofold excess of PPh_3 (Scheme 2), revealing the superior stability of the bisphosphine product over the monophosphine one. In rhodium–phosphine chemistry coordination of single tertiary phosphine is less common, particularly when the corresponding bisphosphine product is formed along the reaction coordinate. It is now of interest to stabilize and isolate the intermediate rhodium compounds coordinated with single phosphine molecule as well as to explore their chemistry during the synthesis of the corresponding bisphosphine product. To the best of our knowledge, only a few instances are reported where monophosphine rhodium precursors are isolated, which ultimately afford more stable bisphosphine analogues in due course of the reaction [1]. The analytical data for these complexes are in good agreement with the above molecular formula. In both the reactions, it has been observed that the HPAN behaves as a bifunctional tridentate ligand.

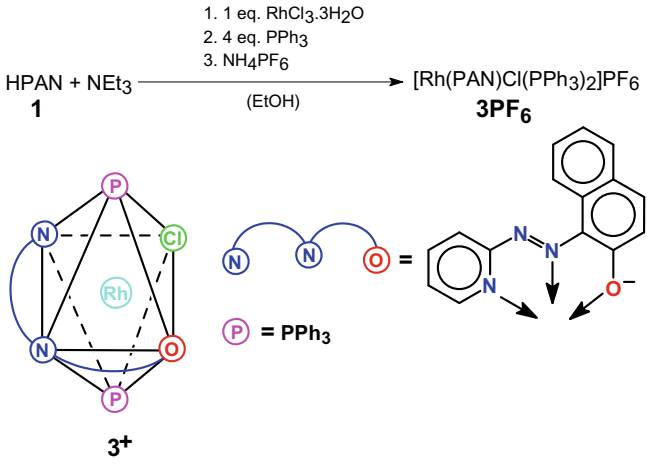

Scheme 1. Synthesis and structure of cationic $[Rh^{III}(PAN)Cl(PPh_3)_2]^+$ complex.

3.2. Crystal structure

The X-ray crystal structures of **3PF$_6$** and **4** were determined to establish the geometries about the metal ions as well as the bonding modes of the PAN and the coligands. Single crystals of the respective complex suitable for X-ray analysis were grown by slow diffusion of hexane into dichloromethane solution at room temperature. Both compounds crystallize in the triclinic space group $P\bar{1}$. The molecular views and atom numbering schemes of these complexes appear in Figs. 1 and 2, respectively. The selected bond distances and angles are given in Table 1. Experimental crystallographic parameters are summarized in Table 2.

The structure of **3PF$_6$** reveals the presence of mononuclear *trans*-$[Rh(PAN)Cl(PPh_3)_2]^+$ cation, hexafluorophosphate anion and one dichloromethane molecule as solvate in the asymmetric unit. In this complex, the central rhodium(III) is surrounded with a N_2OClP_2 distorted octahedral coordination environment by tridentate monoanionic PAN ligand (N, N, O), two *trans*-PPh_3, and one chloride ligands. The title ligand coordinates to rhodium(III) in a meridional fashion using the pyridyl-nitrogen N1, azo-nitrogen

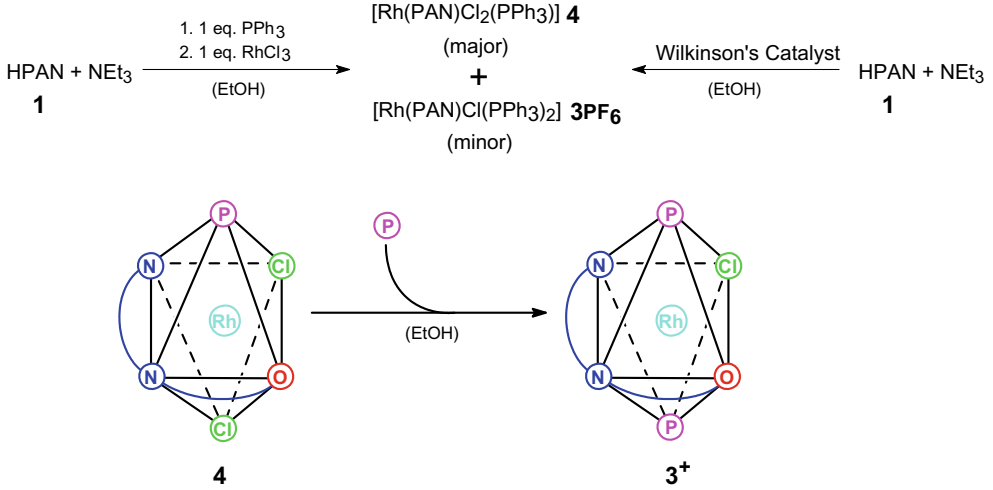

Scheme 2. Synthesis and structure of neutral $[Rh^{III}(PAN)Cl_2(PPh_3)]$ complex and the conversion of **4**–**3$^+$** compound.

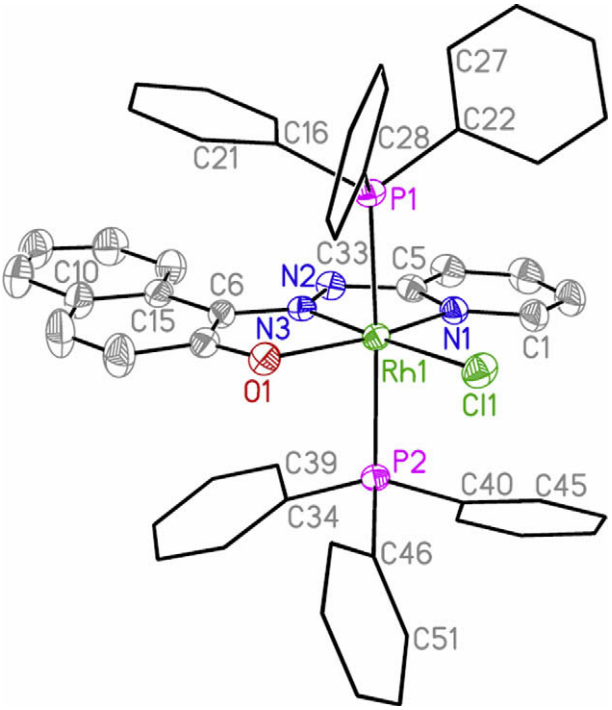

Fig. 1. Molecular structure of **3PF$_6$**. Counter anion (PF_6^-), solvate (CH_2Cl_2) and H atoms are omitted for clarity.

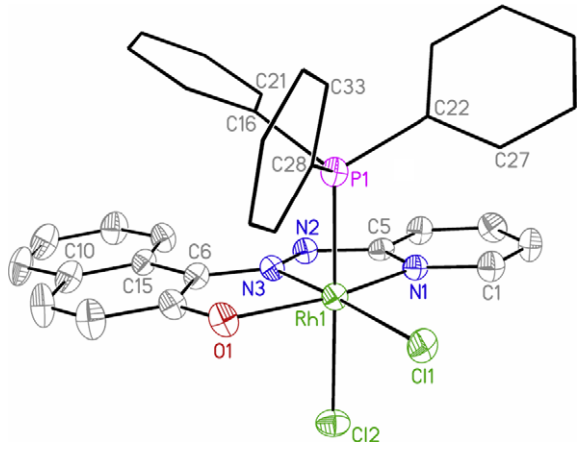

Fig. 2. Molecular structure of **4**. Solvate and H atoms are omitted for clarity.

N3, and naphtholato-oxygen O1 so as to form two adjoining five-membered chelates.

Crystallographic analysis of the neutral complex **4** reveals a distorted octahedral structure with meridional N, N, O coordination of PAN acts as a tridentate monoanionic donor. The coordination sphere of the metal atom is completed by one triphenylphosphine and two *cis*-chloride ligands. The asymmetric unit also contains one CH_2Cl_2 molecule as a solvent of crystallization.

The bond distances (Table 1) indicate strong Rh(d_π)–PAN(p_π) interactions in both complexes. The equatorial plane in pseudooctahedral geometries comprises PAN and one chloride ligand. The mean deviations for the planes including N1, N3, O1 and Cl1 of **3**$^+$ and **4** are 0.022 and 0.026 Å, respectively and for that including the metal atom, N1, N3, O1, Cl1 and Rh1 are 0.018 and 0.030 Å, respectively. Metrical parameters associated with Rh–N(py), Rh–N(azo), Rh–O(naphthalato) and N–N linkages in both complexes

Table 1
Selected bond lengths and angles for **3PF$_6$**·CH_2Cl_2 and **4**·CH_2Cl_2.

Bonds	**3PF$_6$**	**4**
Bond lengths (Å)		
Rh1–N1	2.029(2)	2.012(4)
Rh1–N3	1.945(2)	1.931(4)
Rh1–O1	2.057(2)	2.042(3)
Rh1–P1	2.421(1)	2.293(1)
Rh1–P2	2.389(1)	
Rh1–Cl1	2.385(1)	2.358(1)
Rh1–Cl2		2.374(1)
N2–N3	1.303(3)	1.293(5)
Bond angles (°)		
N1–Rh1–O1	161.12(8)	161.37(14)
N3 – Rh1–Cl1	177.22(6)	175.28(12)
P1–Rh1–P2	174.44(2)	
P1–Rh1–Cl2		176.58(5)
N1–Rh1–N3	79.49(9)	79.95(15)
O1–Rh1–N3	81.70(8)	81.45(14)

Table 2
Crystal data and structure refinement parameters for **3PF$_6$**·CH_2Cl_2 and **4**·CH_2Cl_2.

Parameters	**3PF$_6$**·CH_2Cl_2	**4**·CH_2Cl_2
Empirical formula	$[C_{51}H_{40}ClN_3OP_2Rh]PF_6\cdot CH_2Cl_2$	$C_{33}H_{25}Cl_2N_3OPRh\cdot CH_2Cl_2$
Formula weight	1141.06	769.27
T (K)	273(2)	273(2)
Crystal system	triclinic	triclinic
Space group	$P\bar{1}$	$P\bar{1}$
a (Å)	11.118(2)	10.889(1)
b (Å)	13.600(3)	12.420(1)
c (Å)	17.279(4)	14.137(2)
α (°)	91.01(3)	90.48(1)
β (°)	104.56(3)	104.60(1)
γ (°)	94.01(3)	112.93(1)
Z	2	2
D_{calc} (mg m^{-3})	1.503	1.510
μ (mm^{-1})	0.657	0.900
F(0 0 0)	1156	776
θ Range (°)	1.90–25.00	1.50–25.94
Measured reflections	19 638	16 818
Unique reflections (R_{int})	8798 (0.0165)	6537 (0.0467)
R [$I > 2\sigma(I)$] R_1[a], wR_2[b]	0.0330, 0.0893	0.0514, 0.1261
R (all data) R_1, wR_2	0.0395, 0.0941	0.0880, 0.1454
Goodness-of-fit (GOF) on F^2	1.080	1.040
CCDC No.	703322	703321

[a] $R_1 = \sum|F_o| - |F_c|/\sum|F_o|$.
[b] $wR_2 = [\sum w(F_o^2 - F_c^2)^2/\sum w(F_o^2)^2]^{1/2}$.

are comparable. Nonetheless, several significant features are observed for the mono cationic **3**$^+$ and neutral **4** complexes, notably: (i) the Rh–N(azo) lengths (average 1.938(3) Å) are noticeably shorter by *ca.* 0.08 Å than the Rh–N(py) lengths (average 2.020(3) Å) in both compounds, indicating the stronger Rh(t_2) → N(azo π^*) back donation. (ii) Appreciable elongation of N–N lengths of azo (–N=N–) chromophores (average lengths 1.298(4) Å) in the coordinating ligand, while that in uncoordinated azo ligands lies near 1.25 Å [1,47]. Coordination of PAN to rhodium(III) can lead to a decrease in the N–N bond order due to both σ-donor and π-acceptor character of the ligand, the later character having a more pronounced effect. (iii) Ru1–P1(*trans* to chloride ligand) length of **4** is significantly shorter (~0.11 Å) as compared to the average of Ru–P distances in **3**$^+$ (average 2.405(1) Å) (Table 1),

signifying that $Rh^{III}(t_2) \rightarrow PPh_3(d/\sigma^*)$ back-bonding severely impedes in presence of π-acceptor PPh_3 ligand in the *trans* position. This difference in bond distances is also reflected in the ^{31}P NMR coupling constants, where $^1J_{Rh-P}$ = 115.0 and 87.4 Hz in **4** and $\mathbf{3}^+$, respectively (*vide supra*). (iv) Rh1–Cl1(*trans* to azo) length is shorter by ca. 0.02 Å than Rh1–Cl2(*trans* to PPh_3 ligand) length of **4**, which is attributed to the superior π-acidity vis-à-vis *trans* influence of PPh_3 as compared to azo function [1]. This disparity in bonding pattern between two chloride atoms of **4** is reflected in the notable labileness of Rh1–Cl2(*trans* to PPh_3) bond and explain facile substitution of Cl2 atom with strong π-acid PPh_3 coligand (*vide infra*) during conversion of **4** to $\mathbf{3}^+$. (v) The N, O chelate bite angles of the monoanionic ligand (average 81.6(1)°) are marginally larger than the N, N chelate bite angles of pyridylazo moiety (average 79.7(1)°) in both complexes.

3.3. Spectral studies

3.3.1. IR spectra

Infrared spectra of both the complexes exhibit many sharp and strong vibrations within 1650–400 cm^{-1}. A sharp vibration near 1320 cm^{-1} of the complexes is assigned to the $\nu_{N=N}$. The observed lowering of $\nu_{N=N}$ values by nearly 100 cm^{-1} in complexes as compared to that of **1** is consistent with the Rh(III) → π*(azo) back-bonding [6,30]. Strong bands near 520 and 690 cm^{-1} are indicative of Rh–PPh_3 ligation in the complexes. An additional intense feature at 840 cm^{-1} is observed in the case of $\mathbf{3PF_6}$, which is attributed to the hexafluorophosphate ion.

3.3.2. NMR spectra

The synthesized complexes provide satisfactory elemental analyses and are diamagnetic, which corresponds to the trivalent rhodium (low-spin d^6, $S = 0$) in these complexes. ^1H NMR spectra of these compounds have been recorded in $CDCl_3$ and the spectra are given in the Supplementary data (Fig. S1). The ranges of proton signals for the free HPAN and coordinated PAN ligands appeared almost in the similar region. The aromatic region (δ 6.4–8.9) is rather complex in nature owing to overlap of signals arising from the PPh_3 protons and PAN ligands, of which the most deshielded doublet near 8.8 ppm is assignable to the proton attached with the C1 atom (Figs. 1 and 2). ^1H NMR spectra of both the complexes show multiple signals for the PPh_3 protons within 7.1–7.7 ppm range. Spectra of $\mathbf{3PF_6}$ and **4** show 1:2 and 1:1 relation of ligand/triphenylphosphine signals, respectively; confirming the number of PPh_3 molecule in complexes. Absence of the naphtholic proton signal (appears as a distinct singlet at δ = 15.8 ppm in the free ligand) in complexes authenticates the coordination of naphtholato-O atom. The ^{31}P NMR spectra of the mono and bisphosphine complexes exhibit only single doublet resonances (^{103}Rh nucleus, $I = 1/2$), indicating equivalent phosphine environment (i.e., *trans* dispositions of PPh_3 groups) in the latter compound (Fig. 3). The formation of monophosphine compound **4** results in a significant deshielding (δ ~27 ppm for PPh_3 *trans* to chloride in **4** versus δ ~19 ppm for PPh_3 *trans* to π-acid ligand PPh_3 in $\mathbf{3}^+$) in the ^{31}P signals. The higher $^1J_{Rh-P}$ value of monophosphine compound by ca. 28 Hz in comparison to that of bisphosphine analogue is indicative of the shorter Rh–P length in the former compound (*vide infra*). In $\mathbf{3PF_6}$, a septet pattern is observed at −144 ppm due to the spin–spin coupling of ^{19}F nuclei ($I = 1/2$) with the ^{31}P nucleus, reflecting the presence of PF_6^- as counter anion (Fig. 3).

3.3.3. UV–Vis spectra

Both the complexes are soluble in polar organic solvents such as ethanol, acetonitrile, dichloromethane, chloroform, acetone and so forth, furnishing green solutions but insoluble in hydrocarbon solvents like *n*-hexane, cyclohexane and heptane. The monophosphine intermediate **4** is moderately soluble in nonpolar organic solvents such as benzene and toluene. Electronic spectra of the complexes have been recorded in acetonitrile (Fig. 4) at room tem-

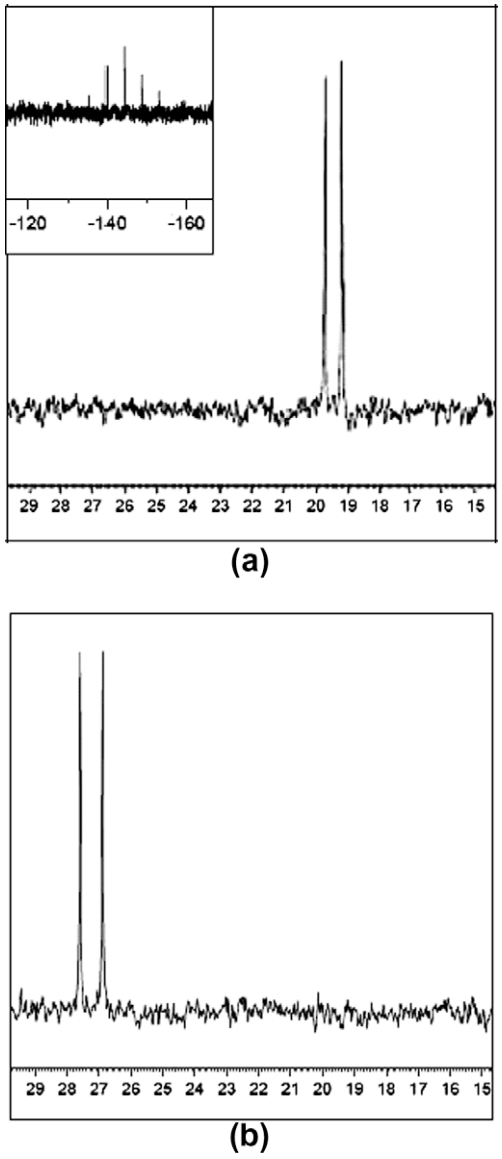

Fig. 3. ^{31}P NMR spectra of (a) cationic complex $\mathbf{3}^+$ and the counter anion $\mathbf{PF_6}^-$ is shown in the inset and (b) neutral complex **4** in $CDCl_3$.

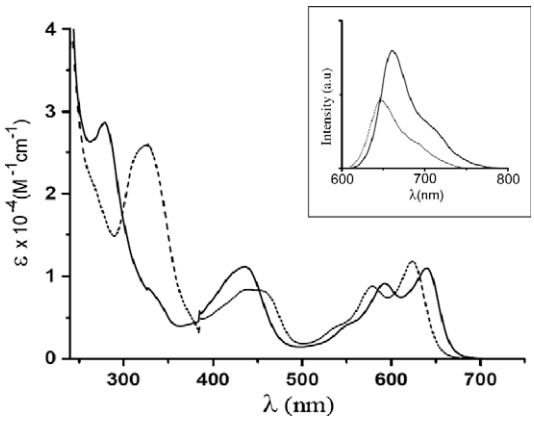

Fig. 4. UV–Vis spectra of $\mathbf{3PF_6}$ (- - - -) and **4** (—) in acetonitrile. Emission spectra of $\mathbf{3PF_6}$ (- - - -) and **4** (—) in acetonitrile are shown in the inset.

Table 3
UV–Vis, emission spectral and cyclic voltammetric data.

Compound	UV–Vis data[a] λ_{max} (nm) (ε, M^{-1} cm^{-1})	Emission spectral data[b] λ_{max} (nm)	Quantum yield (Φ)[c]	Cyclic Voltammetric data[d] (V)
$[Rh(PAN)Cl(PPh_3)_2]PF_6$	624(11 790), 579(8760), 440(8380), 325(25 825)	648	8.3×10^{-4}	1.08[e], −0.48[f]
$[Rh(PAN)Cl_2(PPh_3)]$	640(10 950), 593(9120), 436(11 150), 278(28 596)	661	1.6×10^{-3}	1.60[e], −0.54[f]

[a] In acetonitrile.
[b] In acetonitrile, excitation at 580 nm.
[c] In deoxygenated acetonitrile.
[d] Solvent, acetonitrile; supporting electrolyte, TEAP; reference electrode Ag/AgCl; scan rate, 50 mV s^{-1}.
[e] Anodic peak potential (E_{pa}) value.
[f] Cathodic peak potential (E_{pc}) value.

perature. Multiple low-energy transitions are the characteristics of the spectra (Table 3) and these excitations are believed to be due to charge-transfer transitions involving the three-coordinated 2-(pyridylazo)naphtholate and other coligand orbitals. The spectral patterns of the compounds are similar except the slight hypsochromic shift of the low-energy excitations (550–650 nm) by ca. 15 nm in case of **$3PF_6$** relative to **4**, which is ascribed to the weaker charge-transfer transitions upon second phosphine coordination. Notably, the low-energy transitions in rhodium(III) complexes are less common [6,48] and may have usefulness with regard to the development of photocatalysts active in the long-wavelength region of the visible spectrum. To gain insight into the nature of FMOs, we performed Density Functional Theory (DFT) calculations with the crystallographic parameters. The isodensity plot from HOMO−1 to LUMO+1 for **$3PF_6$** and **4** is illustrated in Fig. 5 and composition of these molecular orbitals is given in Table S1. The calculations have indicated that the top three occupied orbitals (HOMO, HOMO−1 and HOMO−2) as well as low-energy acceptor orbitals (LUMO, LUMO+1, LUMO+2) in both the complexes are predominantly centered on PAN ligand and coligand (Cl and PPh_3) orbitals with only small contributions from the metal orbitals. The HOMO of **$3PF_6$** consists principally of a mixture of PAN-π and phenyl-π of PPh_3, and that of **4** is localized largely on PAN-π and Cl-p orbitals; with major contribution (∼75%) from the PAN ligand in both cases. LUMO for both the compounds are distributed almost exclusively (∼90%) over the three-coordinated PAN ligand. Significantly, Rh-d orbitals appear to contribute very little electron density to either the HOMO or LUMO. Additionally, presence of low-energy MLCT and LMCT states are unexpected for these compounds since Rh(III) is rather redox inert [49]. These results tempt us to propose that these low-energy transitions involve orbitals that are predominantly ligand in character and originated primarily from the coordinated PAN ligand part.

3.3.4. Emission spectra

Rhodium(III) polyazine complexes have been extensively studied for their photophysical property in recent years though they usually do not exhibit photoluminescence at room temperature [50–56]. To the best of our knowledge, no report about photoluminescence of rhodium(III)–PAN (a typical azo-imine kind of ligand) compounds is documented in the literature. Here we present the room temperature photoluminescence spectra for both rhodium(III)–PAN compounds (Table 3). The complexes **$3PF_6$** and **4** are luminescent in acetonitrile solution with a broad emission band centered at $\lambda = 648$ nm ($\Phi = 8.3 \times 10^{-4}$) and $\lambda = 661$ nm ($\Phi = 1.6 \times 10^{-3}$), respectively, after excitation at $\lambda = 580$ nm. Emission quantum yields were determined at 25 °C in deoxygenated acetonitrile solution (argon bubbling for 30 min) with cresyl violet perchlorate in methanol as a standard ($\Phi_r = 0.54$) [57]. The emission quantum yield for complexes (Φ_u) was calculated by the well-known equation given below:

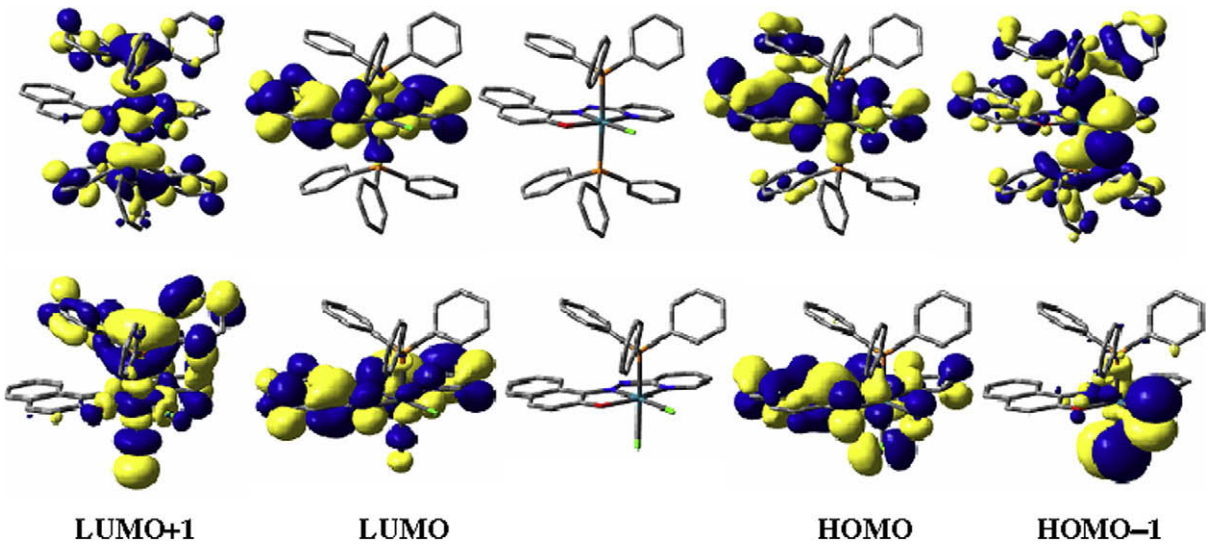

Fig. 5. Selected FMOs of **$3PF_6$** (top) and **4** (bottom) (isosurface cutoff value = 0.02). Color code for atom: grey, C; blue, N; orange, P; red, O; green, Cl; aquamarine, Rh. (For interpretation of the references to color in this figure legend, the reader is referred to the web version of this article.)

$$\Phi_u = \Phi_r(A_r/A_u)(I_u/I_r)(n_u/n_r)^2 \quad (1)$$

where A_u, A_r are the absorption values of unknown and reference; I_u, I_r are the integrated emission areas of unknown and reference; and n_u, n_r are the refractive indices of the solvents containing unknown and reference [58]. The experimental red emission spectra are depicted in the inset of Fig. 4. Notably, platinum group metal–phosphine complexes hardly show emissive property at room temperature [59], the synthesized complexes do emit. Nonetheless, the emission intensity decreases in presence of PPh_3 group as the monophosphine derivative **4** appears to be nearly doubly emissive relative to bisphosphine compound **3PF$_6$**. MLCT character of the emission process is rather unlikely since Rh(III) is redox inert system [60]. Although the nature of the emission level of these rhodium(III)–PAN compounds is not obvious, but can be attributed to an ILCT level involving the donor and acceptor moieties of the PAN ligand [55,56,61].

3.4. Ligand redox

Electron-transfer property of the rhodium(III)–PAN complexes has been studied by using cyclic voltammetry in acetonitrile (~0.1 M NEt_4ClO_4) by using a platinum working electrode and the reported potentials are referenced to the Ag/AgCl electrode. Voltammetric data are presented in Table 3 and the voltammograms are shown in Fig. 6. The value for the ferrocenium/ferrocene couple, under our experimental conditions, was 0.52 V. Both complexes show an oxidative response and the voltammograms are irreversible in nature. The one-electron nature of the oxidation processes has been verified by comparing theirs current height (i_{pa}) with that of the standard ferrocenium/ferrocene couple under identical experimental conditions. It is very likely that this process corresponds to the oxidation of the three-coordinated 1-(2′-pyridylazo)-2-naphtholate ligand (Eq. (2) and (3)). The oxidative response can be assigned primarily

$$[Rh^{III}(PAN^{-I})Cl(PPh_3)_2]^+ - e^- \rightarrow [Rh^{III}(PAN)Cl(PPh_3)_2]^{2+} : \text{for } \mathbf{3}^+ \quad (2)$$

$$[Rh^{III}(PAN^{-I})Cl_2(PPh_3)] - e^- \rightarrow [Rh^{III}(PAN)Cl_2(PPh_3)]^+ : \text{for } \mathbf{4} \quad (3)$$

to a ligand-centered redox process [26]. In addition, both complexes show one-electron irreversible reduction waves (E_{pc}) near −0.5 V versus Ag/AgCl. These responses are believed to be centered on the coordinated azo ligand (Fig. 5) [1,2]. The cyclic voltammogram of neutral HPAN exhibits irreversible reductive response at −1.33 V versus Ag/AgCl corresponds to azo reduction of the free ligand. Analogous reduction of azo π^* MO of other free ligands incorporating "pyridylazo" moiety were observed near −1.30 V [62,63]. In complexes the azo reduction occurs at more positive potentials than in uncoordinated HPAN reflecting the expected stabilization of the π^* MO upon coordination [62]. The redox noninnocence of PAN is supported by the theoretical study where HOMOs as well as LUMOs are almost exclusively distributed over the PAN ligand for both compounds (*vide infra*).

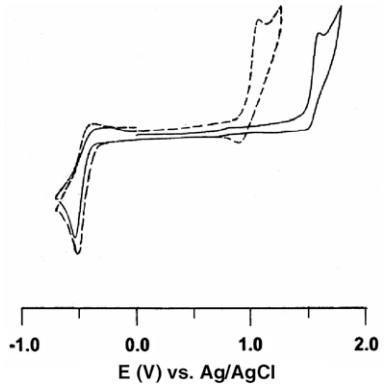

Fig. 6. Cyclic voltammograms of **3PF$_6$** (- - - -) and **4** (—) in acetonitrile (0.1 M TEAP) at a scan rate of 50 mV s^{-1}.

4. Conclusion

In this work, mononuclear Rh(III) complex of PAN of the type *trans*-$[Rh(PAN)Cl(PPh_3)_2]PF_6$ (PAN = NNO donor azo ligand) is reported. We were also able to isolate the intermediate *cis*-$[Rh(PAN)Cl_2(PPh_3)]$ with 1 equivalent of PPh_3 relative to both **1** and $RhCl_3{\cdot}3H_2O$. Both the complexes were characterized by various spectral techniques and their structures were authenticated by X-ray crystallography. The title ligand behaves as a tridentate monoanionic N,N,O-donor and shows strong affinity toward Rh(III), indicating its overall borderline nature. The complexes thus formed show rich spectral as well as redox properties, which have been thoroughly investigated. Most notable is the appearance of absorption and luminescence in the low-energy part of the visible region. Remarkably, the rhodium(III)–PAN complexes show red luminescence in solution at room temperature. The redox orbitals of both compounds are supposed to be centered on coordinated PAN ligand.

Acknowledgements

We thank the Department of Science and Technology, New Delhi, for financial assistance (Grant SR/FTP/CS-20/2005). We also thank the Department of Chemistry, IIT Guwahati and DST-funded National Single Crystal X-ray diffraction Facility at the Department of Inorganic chemistry, IACS for X-ray data collections. Financial assistance received from the UGC-CAS program in the Department of Chemistry, Jadavpur University is acknowledged. We thank Dr. K.K. Rajak, Department of Chemistry, Jadavpur University for help in computations. B. Adhikari thanks the UGC, New Delhi, for his fellowship.

Appendix A. Supplementary data

CCDC 703322 and 703321 contain the supplementary crystallographic data for **3PF$_6$**·CH_2Cl_2 and **4**·CH_2Cl_2. These data can be obtained free of charge via http://www.ccdc.cam.ac.uk/conts/retrieving.html, or from the Cambridge Crystallographic Data Centre, 12 Union Road, Cambridge CB2 1EZ, UK; fax: (+44) 1223-336-033; or e-mail: deposit@ccdc.cam.ac.uk. ^{1}H NMR spectra (Fig. S1) and composition of frontier molecular orbitals (Table S1 and S2) of **3PF$_6$** and **4** are given. Supplementary data associated with this article can be found, in the online version, at doi:10.1016/j.poly.2009.12.001.

References

[1] K. Pramanik, U. Das, B. Adhikari, D. Chopra, H. Stoeckli-Evans, Inorg. Chem. 47 (2008) 429–438.
[2] S. Dutta, S.-M. Peng, S. Bhattacharya, J. Chem. Soc., Dalton Trans. (2000) 4623–4627.
[3] S. Baksi, R. Acharyya, F. Basuli, S.-M. Peng, G.-H. Lee, M. Nethaji, S. Bhattacharya, Organometallics 26 (2007) 6596–6603.
[4] J. Pratihar, N. Maiti, S. Chattopadhyay, Inorg. Chem. 44 (2005) 6111–6114.
[5] J. Pratihar, D. Patra, S. Chattopadhyay, J. Organomet. Chem. 690 (2005) 4816–4821.
[6] C. Das, A.K. Ghosh, C.-H. Hung, G.-H. Lee, S.-M. Peng, S. Goswami, Inorg. Chem. 41 (2002) 7125–7135.
[7] A.K. Ghosh, P. Majumdar, L.R. Falvello, G. Mostafa, S. Goswami, Organometallics 18 (1999) 5086–5090.
[8] J.R. Stokely, W.D. Jacobs, Anal. Chem. 35 (1963) 149–152.
[9] Y. Shijo, K. Nakaji, T. Shimizu, Analyst 113 (1988) 519–521.

[10] E.M. Basova, T.A. Boĺshova, V.M. Ivanov, J. Anal. Chem. 52 (1997) 647–655 (translation of Zh. Anal. Khim.).
[11] N. Shokoufi, F. Shemirani, Talanta 73 (2007) 662–667.
[12] A.E. Tschitschibabin, J. Russ. Phys. Chem. Soc. 47 (1915) 1582.
[13] A.E. Tschitschibabin, J. Russ. Phys. Chem. Soc. 50 (1918) 513–516.
[14] K.L. Cheng, R.H. Bray, Anal. Chem. 27 (1955) 782–785.
[15] D. Betteridge, D. John, Analyst 98 (1973) 390–411.
[16] W.W. White, P.J. Murphy, Anal. Chem. 47 (1975) 2054–2057.
[17] E.P. Benson, J.I. Legg, Inorg. Chem. 20 (1981) 2504–2507.
[18] R.L. Reeves, G.S. Calabrese, S.A. Harkaway, Inorg. Chem. 22 (1983) 3076–3084.
[19] S.A. Morozko, V.M. Ivanov, J. Anal. Chem. 50 (1995) 572–578 (transl. of Zh. Anal. Khim.).
[20] L.G. Hargis, J.A. Howell, R.E. Sutton, Anal. Chem. 68 (1996) 169R–183R.
[21] J.A. Howell, Anal. Chem. 70 (1998) 107R–118R.
[22] D. Bohrer, P.C. Nascimento, M. Guterres, M. Trevisan, E. Seibert, Analyst 124 (1999) 1345–1350.
[23] S. Ooi, D. Carter, Q. Fernando, Chem. Commun. (1967) 1301–1302.
[24] H. Adams, R.M. Bucknall, D.E. Fenton, M. Garcia, J. Oakes, Polyhedron 17 (1998) 4169–4177.
[25] M.S. Sastry, U.P. Singh, Cryst. Res. Technol. 24 (1989) K148–K151.
[26] S. Basu, S. Halder, I. Pal, S. Samanta, P. Karmakar, M.G.B. Drew, S. Bhattacharya, Polyhedron 27 (2008) 2943–2951.
[27] B. Machura, J. Mroziński, R. Kruszynski, J. Kusz, Polyhedron 27 (2008) 3013–3019.
[28] R.A. Krause, K. Krause, Inorg. Chem. 21 (1982) 1714–1720.
[29] S. Goswami, R. Mukherjee, A. Chakravorty, Inorg. Chem. 22 (1983) 2825–2832.
[30] J.J. Robertson, A. Kadziola, R.A. Krause, S. Larsen, Inorg. Chem. 28 (1989) 2097–2102.
[31] J.E. Huheey, E.A. Keiter, R.L. Keiter, Inorganic Chemistry: Principles of Structure and Reactivity, forth ed., Harper Collins College Publishers, New York, 1993. p. 421.
[32] M. Velusamy, M. Palaniandavar, R.S. Gopalan, G.U. Kulkarni, Inorg. Chem. 42 (2003) 8283–8293.
[33] F.H. Jardine, P.S. Sheridan, Rhodium, in: G. Wilkinson, R.D. Gillard, J.A. McCleverty (Eds.), Comprehensive Coordination Chemistry, vol. 4, Springer, New York, 1987, p. 930.
[34] J.A. Osborn, G. Wilkinson, Inorg. Synth. 10 (1967) 67–70.
[35] G.M. Sheldrick, SHELXS-97, Program for Crystal Structure Solution, University of Göttingen, Germany, 1997.
[36] G.M. Sheldrick, SHELXL-97, Program for Refining X-ray Crystal Structures, University of Göttingen, Germany, 1997.
[37] G.M. Sheldrick, SHELXTL, v. 6.14, Bruker AXS Inc., Madison, WI, 2003.
[38] C.K. Johnson, ORTEP, Report ORNL-5138, Oak Ridge National Laboratory, Oak Ridge, TN, 1976.
[39] R.G. Parr, W. Yang, Density-Functional Theory of Atoms and Molecules, Oxford University Press, Oxford, UK, 1989.
[40] A.D. Becke, J. Chem. Phys. 98 (1993) 5648–5652.
[41] C. Lee, W. Yang, R.G. Parr, Phys. Rev. B 37 (1998) 785–789.
[42] M.J. Frisch, G.W. Trucks, H.B. Schlegel, G.E. Scuseria, M.A. Robb, J.R. Cheeseman, J.A. Montgomery Jr., T. Vreven, K.N. Kudin, J.C. Burant, J.M. Millam, S.S. Iyengar, J. Tomasi, V. Barone, B. Mennucci, M. Cossi, G. Scalmani, N. Rega, G.A. Petersson, H. Nakatsuji, M. Hada, M. Ehara, K. Toyota, R. Fukuda, J. Hasegawa, M. Ishida, T. Nakajima, Y. Honda, O. Kitao, H. Nakai, M. Klene, X. Li, J.E. Knox, H.P. Hratchian, J.B. Cross, V. Bakken, C. Adamo, J. Jaramillo, R. Gomperts, R.E. Stratmann, O. Yazyev, A.J. Austin, R. Cammi, C. Pomelli, J.W. Ochterski, P.Y. Ayala, K. Morokuma, G.A. Voth, P. Salvador, J.J. Dannenberg, V.G. Zakrzewski, S. Dapprich, A.D. Daniels, M.C. Strain, O. Farkas, D.K. Malick, A.D. Rabuck, K. Raghavachari, J.B. Foresman, J.V. Ortiz, Q. Cui, A.G. Baboul, S. Clifford, J. Cioslowski, B.B. Stefanov, G. Liu, A. Liashenko, P. Piskorz, I. Komaromi, R.L. Martin, D.J. Fox, T. Keith, M.A. Al-Laham, C.Y. Peng, A. Nanayakkara, M. Challacombe, P.M.W. Gill, B. Johnson, W. Chen, M.W. Wong, C. Gonzalez, J.A. Pople, GAUSSIAN 03, Revision C.02, Gaussian Inc., Wallingford CT, 2004.
[43] P.J. Hay, W.R. Wadt, J. Chem. Phys. 82 (1985) 270–283.
[44] P.J. Hey, W.R. Wadt, J. Chem. Phys. 82 (1985) 299–310.
[45] G.L. Miessler, D.A. Tarr, Inorganic Chemistry, second ed., Pearson, Prentice Hall, 2000. p. 174.
[46] M. Shivakumar, K. Pramanik, I. Bhattacharyya, A. Chakravorty, Inorg. Chem. 39 (2000) 4332–4338.
[47] K. Pramanik, M. Shivakumar, P. Ghosh, A. Chakravorty, Inorg. Chem. 39 (2000) 195–199.
[48] F.A. Cotton, G. Wilkinson, C.A. Murillo, M. Bochmann, Advanced Inorganic Chemistry, sixth ed., Wiley, New York, 1999. p. 1048.
[49] A.B.P. Lever, Inorganic Electronic Spectroscopy, Elsevier, Amsterdam, 1984.
[50] M. Nishizawa, T.M. Suzuki, S. Sprouse, R.J. Watts, P.C. Ford, Inorg. Chem. 23 (1984) 1837–1841.
[51] D. Loganathan, J.H. Rodriguez, H. Morrison, J. Am. Chem. Soc. 125 (2003) 5640–5641.
[52] D. Amarante, C. Cherian, A. Catapano, R. Adams, M.H. Wang, E.G. Megehee, Inorg. Chem. 44 (2005) 8804–8809.
[53] M.C. Tseng, J.L. Ke, C.C. Pai, S.P. Wang, W.L. Huang, Polyhedron 25 (2006) 2160–2166.
[54] K. Dedeian, J. Shi, E. Forsythe, D.C. Morton, Inorg. Chem. 46 (2007) 1603–1611.
[55] M.T. Indelli, C. Chiorboli, L. Flamigni, L.D. Cola, F. Scandola, Inorg. Chem. 46 (2007) 5630–5641.
[56] J.B. Waern, C. Desmarets, L.M. Chamoreau, H. Amouri, A. Barbieri, C. Sabatini, B. Ventura, F. Barigelletti, Inorg. Chem. 47 (2008) 3340–3348.
[57] D. Magde, J.H. Brannon, T.L. Cremers, J. Olmsted III, J. Phys. Chem. 83 (1979) 696–699.
[58] J.R. Lakowicz, Principles of Fluorescence Spectroscopy, third ed., Springer, New York, 2006. pp. 54–55.
[59] J.V. Caspar, T.J. Meyer, Inorg. Chem. 22 (1983) 2444–2453.
[60] H. Kunkely, A. Vogler, Chem. Phys. Lett. 319 (2000) 486–488.
[61] L. Ghizdavu, O. Lentzen, S. Schumm, A. Brodkorb, C. Moucheron, A.K.-D. Mesmaeker, Inorg. Chem. 42 (2003) 1935–1944.
[62] M.N. Ackermann, C.R. Barton, C.J. Deodene, E.M. Specht, S.C. Keill, W.E. Schreiber, H. Kim, Inorg. Chem. 28 (1989) 397–403.
[63] M. Krejčík, S. Záliš, J. Klíma, D. Sýkora, W. Matheis, A. Klein, W. Kaim, Inorg. Chem. 32 (1993) 3362–3368.